JOURNAL OF GEOPHYSICAL RESEARCH, VOL. 102, NO. C11, PAGES 25,061–25,071, NOVEMBER 15, 1997

Effects of a sewage plume on the biology, optical characteristics, and particle size distributions of coastal waters

A. A. Petrenko,[1,2] B. H. Jones,[3] T. D. Dickey,[4] M. LeHaitre,[5] and C. Moore[6]

Abstract. The effect of a sewage plume on the biology, optical characteristics, and particle size distributions of coastal waters was evaluated around the Sand Island, Hawaii, outfall diffuser. In situ physical and biooptical data and Niskin bottle samples were collected during a 1-week cruise from September 25 to October 1, 1994. One or two layers affected by sewage could be distinguished in the water column: recently discharged ("new") sewage plume waters and "old" plume waters. In conditions characterized by high Froude number the distribution of chlorophyll fluorescence in new plume waters was the same as for ambient waters, while for low Froude number, chlorophyll fluorescence increased within the plume, demonstrating the importance of physical forcing on effluent and phytoplankton interactions. New plume waters were associated with at least 2.7-fold increases in particle load, high concentrations of particles larger than 70 μm, increases in ammonium, phosphate, and silicate, and high levels of heterotrophic bacteria and *Prochlorococcus* compared to surrounding waters. Both new and old plume layers, but not phytoplankton layers, showed distinct increases in fluorescence for the excitation/emission (Ex/Em) wavelength pair Ex/Em = 228/340 in nm, interpreted as particulate tryptophan-like fluorescence. Such fluorescence may be useful as a new in situ real-time indicator of waters affected by effluent discharges.

1. Introduction

Coastal waters surrounding many major metropolitan areas receive substantial inputs of nutrients and contaminants from treated wastewaters discharged by offshore outfall diffusers. The goal of diffuser design and placement is to minimize the negative impacts of injected wastewaters on human populations. These impacts include, but are not limited to, direct contact (e.g., by swimmers, surfers, beachgoers) with chemical contaminants or pathogens and indirect effects through the consumption of contaminated food supplies (e.g., fish, shellfish). However, even if the negative impacts on human populations are minimized, the effects of the plume on the local ecosystem may still be substantial. The fate of injected effluent depends upon a variety of physical and biological processes, some of which are intimately coupled to the concentration, content, and mixing of wastewater with surrounding water masses. Coastal physical and biological processes are highly dynamic and complex and are, in most instances, poorly understood. Consequently, how sewage disperses and how effluent modifies and is modified by coastal biota remain in many respects unknown and unpredictable.

Sewage treatment is designed to remove most suspended solids and biological oxygen demand (BOD), leaving nutrient input as one of the most significant remaining problems. The high concentrations of nutrients in a sewage plume, as well as the remaining BOD, cause disruptions that range from increases in phytoplankton biomass to harmful algal blooms and eutrophication problems [*Laws*, 1993]. Additionally, even after treatment, wastewater still contains some toxic substances, including metal contaminants and pathogens. The most traditional and widespread technique to determine the effects of effluent on the biology of the waters into which it is discharged is based on bottle or benthic sampling. Samples are brought back to a land-based laboratory and analyzed for fecal bacteria, nutrients, algal composition, metal contamination, etc. Such postcollection sample analysis provides key information on plume effects, but it lacks high spatial and temporal resolution and does not permit real-time detection of the sewage plume.

An important goal of modern plume studies is the development of in situ real-time detection techniques for monitoring sewage plumes. Detection of wastewater can be accomplished using the natural tracers associated with the effluent [*Jones et al.*, 1990, 1991, 1993; *Washburn et al.*, 1992; *Wu et al.*, 1994], acoustic backscatter measurements [e.g., *Besiktepe et al.*, 1995; *Dammann et al.*, 1991], or introduced tracer techniques (among the most recent studies, *Davison et al.* [1993], *Faisst et al.* [1990], *Parnell* [1992], and *Roberts and Wilson* [1990]). Nonetheless, a reliable in situ real-time technique is still sought [*Petrenko*, 1997]. Newly developed multiwavelength instruments, such as absorption-attenuation sensors (e.g., ac-9), backscatter sensors, and fluorometers (e.g., SAFire) are now able to measure spectral inherent optical properties or fluorescence in

[1]Department of Earth Sciences, University of Southern California, Los Angeles.
[2]Now at College of Atmospheric and Oceanic Sciences, Oregon State University, Corvallis, Oregon.
[3]Department of Biological Sciences, University of Southern California, Los Angeles.
[4]Institute for Computational Earth System Science, University of California Santa Barbara.
[5]Institut Francais de Recherche pour l'Exploitation de la Mer, Brest.
[6]Western Environmental Technology Laboratories Inc., Philomath, Oregon.

Paper number 97JC02082.
0148-0227/97/97JC-02082$09.00

situ. Such measurements may exhibit specific optical characteristics associated with sewage plumes, which could be used as optical tracers of sewage. To take advantage of this new generation of instruments, the optical characteristics of wastewater must be known.

Only a few studies on the absorption and fluorescence of both raw and treated sewage have appeared in the peer-reviewed literature [*Ahmad et al.*, 1993; *Ahmad and Reynolds*, 1995; *Reynolds and Ahmad*, 1995]. Absorption spectra of raw sewage exhibit a local maximum at 280 nm, which is absent in absorption of secondary-treated wastewater [*Ahmad et al.*, 1993]. Raw sewage fluorescence varies in magnitude from sample to sample but exhibits an approximately constant spectral shape [*Ahmad et al.*, 1993]. *Ahmad et al.* [1993] found that two chromophoric groups are excited at 248 nm in raw sewage (one with an emission maximum around 340 nm, the other around 370 nm). *Ahmad and Reynolds* [1995] attributed such peaks to biodegradable aromatic hydrocarbon constituents, present in both raw and secondary-treated sewage samples. They asserted that since the peak positions were highly reproducible in samples from different locations and times, such a technique could potentially be used for estimating concentrations of biodegradable constituents and suspended solids in wastewaters.

Mamala Bay, the southern bay of Oahu, Hawaii, displays a complex oceanographic environment into which anthropogenic particle fields are introduced. Municipal wastewater is discharged, after primary treatment, through the Sand Island Treatment Plant (SITP) sewage outfall located 4 km offshore at the top of the continental slope, where flushing with offshore waters is expected. Pollution problems occurring throughout the year on the eastern beaches of Mamala Bay prompted a general study of all potential point and nonpoint sources of pollution in the bay [*Colwell et al.*, 1995]. Data for the present study were collected as part of the component of the Mamala Bay project focusing on the SITP sewage plume.

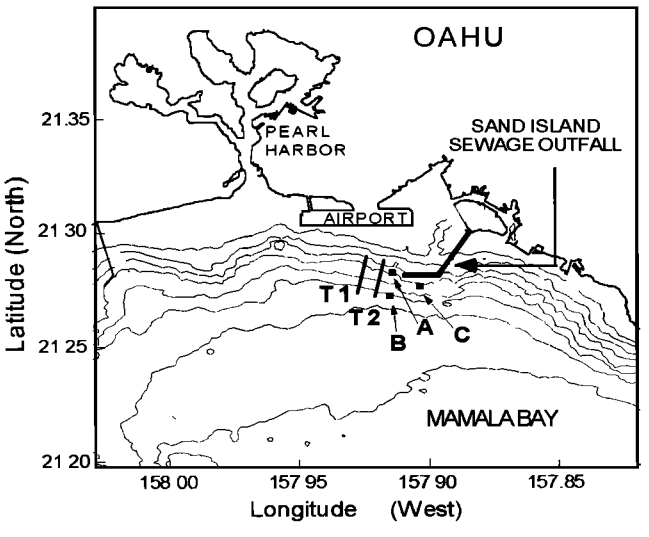

Figure 1. Map of the eastern part of Mamala Bay. Casts 9, 13, and 19 were collected at station A; cast 12 at station B; and cast 15 at station C. Towyo 30 was collected along T1, and towyo 32 along T2. Isobaths correspond to depths of 15, 25, 50, 100, 200, 300, 400, and 500 m.

Table 1. Subset of Data Selected for the Study

Casts/Towyo	Location in Figure 1	Date	Time (UT)
Cast 9	station A	Sept. 29	1700
Cast 12	station B	Sept. 29	1900
Cast 13	station A	Sept. 30	0930
Cast 15	station C	Sept. 30	1330
Towyo 30	T1	Oct. 01	1010-1025
Towyo 32	T2	Oct. 01	1115-1130
Cast 19	station A	Oct. 01	1300

The primary goal of this study was to determine the effects of the SITP sewage plume on the biology, optical characteristics, and particle size distributions using a natural tracer technique, state-of-the-art in situ instruments (ac-9, SAFire, and particle size analyzer), and bottle sample analyses. The secondary goal was to evaluate the potential of new in situ real-time techniques for detecting effluent-affected waters.

2. Methods

The present field study took place aboard the R/V *Kila* from September 25 to October 1, 1994. The sampling region was approximately 6 km along-shore and 3 km cross-shelf centered on the Sand Island outfall diffuser (Figure 1). In situ measurements were obtained from an instrumented towyo platform executing either vertical profiles (referred to as casts) or towyos. Details on the casts and towyos corresponding to the subset of data used in this study are given in Table 1. Data were time-stamped (for postcruise merging of the data) and recorded simultaneously via the modular ocean data acquisition power system (MODAPS, WETLabs, Inc.). Following vertical profiling with the towyo instrument package, discrete water samples were obtained with 5-L Niskin bottles at selected depths based on features apparent in the vertical profiles. Undiluted, treated sewage samples were directly collected at the SITP, in the open basin leading to the underwater outfall, on three occasions (September 29, 0745 UT; September 30, 1640 UT; and October 5, 0930 UT). The various parameters derived from data, measured either in situ or in the laboratory, are described below.

2.1. Physical Data

Conductivity, temperature (°C), and pressure (dbar), were measured with a conductivity-temperature-depth (CTD) instrument (Sea-Bird Electronics model SBE 9/11+), and were used to derive salinity (practical salinity units, psu).

2.2. Inherent Optical Properties

Some inherent optical properties (IOPs) were measured in situ as continuous profiles or at discrete depths from bottle samples.

2.2.1. In situ IOPs. The in situ instruments included a 0.25 m path length transmissometer at 660 nm wavelength (Sea Tech, Inc.), providing the beam attenuation coefficient at 660 nm (c660 in m^{-1}; which includes pure water attenuation), and a nine-wavelength absorption-attenuation meter (ac-9, WETLabs, Inc.), providing absorption and beam attenuation coefficients (a_{meas} and c; pure water subtracted). The ac-9

wavelengths were 412, 440, 488, 510, 560, 630, 650, 676, and 715 nm (all bandwidths were 10 nm full width at half maximum (FWHM)) [*Moore et al.*, 1992]. The 560 nm data were omitted, since ac-9 postcruise calibration showed a deficient filter at that wavelength. Absorption at 715 nm was corrected for temperature variations, according to

$$a_c(715) = a_{meas}(715) - 0.0025(T - T_{cal})$$

where T is the in situ measured temperature and T_{cal} the ac-9 calibration temperature [*Pegau*, 1996]. Salinity corrections had a negligible effect on the data. Absorption coefficient (a) was obtained after correction for scattering:

$$a(\lambda) = a_{meas}(\lambda) - a_c(715)\frac{c(\lambda) - a(\lambda)^*}{c(715) - a_c(715)}$$

where $a(\lambda)^* = a_{meas}(\lambda)$ for $\lambda < 715$ nm and $a(715)^* = a_c(715)$ [*Zaneveld et al.*, 1994]. This scattering correction for the absorption coefficient assumed no absorption at 715 nm. Scattering coefficient (b) was calculated by difference between c and a ($b = c - a$).

2.2.2. Absorption from bottle samples. Particulate, detrital, and dissolved organic matter (DOM) absorptions were obtained at discrete depths from seawater samples. Samples were filtered through Whatman GF/F glass-fiber filters, and filters were frozen in liquid nitrogen. Frozen filters were kept at -20°C for up to 7 days, and filtrates were refrigerated not more than 13 days before laboratory spectrophotometer analysis. In the laboratory, particulate, detrital, and filtrate absorption spectra were run on an HP 8452A diode array spectrophotometer (a Labsphere RSA-HP-84 integrating sphere was used for filtrate absorption).

Particulate absorption spectra were determined using the filter pad technique [e.g., *Mitchell and Kiefer*, 1984] from 350 to 750 nm with 2 nm resolution. The absorption coefficient of particulate matter, a_p (in units of m^{-1}), was calculated as

$$a_p(\lambda) = \frac{2.303 A_p(\lambda) S}{V \beta}$$

where A_p is the absorbance measured by the spectrophotometer, 2.303 is the factor converting base 10 to a natural logarithm, S is the clearance area of the filter, V is the volume of seawater filtered, and β is the spectral amplification factor correcting for scattering within the glass-fiber filter [*Bricaud and Stramski*, 1990; *Mitchell and Kiefer*, 1988]. Filters were then soaked in 20 mL of hot methanol for 45 min and rinsed with distilled water [*Kishino et al.*, 1985]. Hot methanol extracts pigments and leaves on the filter not only the unpigmented particles but also bleached cells and nonextractable pigments; it also extracts detrital carotenoids and extractable pheopigments that belong to the detrital phase retained on the filter. Absorption spectra, after methanol extraction, are referred to as detrital absorption spectra, despite the addition or absence of the constituents mentioned above. Detrital absorption was calculated in the same way as a_p

For filtrate samples, scans were made from 280 to 800 nm with 2 nm resolution using a 10-cm path length quartz cuvette. Filtration with GF/F glass-fiber filters allows particles smaller than approximately 0.7 μm to pass through. Nonetheless, filtrate absorption spectra will be referred to hereafter as DOM spectra, although filtrates contained the small particles that passed through. The DOM absorption coefficient was calculated as

$$a_{DOM}(\lambda) = \frac{2.303 A_{DOM}(\lambda)}{l}$$

where A_{DOM} is the absorbance measured by the spectrophotometer and l is the cuvette path length (0.1 m here).

For all three methods, baselines were scanned at regular intervals with blanks, which were either unused filters soaked in distilled water (DH_2O) for a_p and detrital absorption (a_d), or DH_2O in the sample cuvette for a_{DOM}. Baseline uncertainties in DOM measurements prevented absolute DOM determinations. Hence relative DOM measurements were used when possible. For example, two depths (10 and 55 m) at cast 9 had DOM spectra with identical baselines, so relative DOM absorption between 55 and 10 m was calculated. Relative total absorption, a_t, was calculated as the sum of relative a_p and relative a_{DOM} between depths where relative a_{DOM} data were available.

2.3. Fluorescence

Fluorescence was measured in situ with two instruments, the Sea Tech, Inc. chlorophyll-sensitive fluorometer [*Bartz et al.*, 1988] and the spectral absorption and fluorescence instrument (SAFire, WETLabs, Inc.).

The Sea Tech fluorometer has an excitation range centered at 425 nm, 200 nm FWHM, and emission at 685 nm, 30 nm FWHM. Chlorophyll fluorescence (in arbitrary units (a.u.)) was compared with the fluorescence emitted by chlorophyll and pheopigments (assuming that chlorophyll fluoresces 2.2 times more than pheopigments [*Holm-Hansen et al.*, 1965]). The conversion factor was found to vary both with depth and time, so no systematic calibration of the chlorophyll fluorescence could be done and results are presented in arbitrary units.

The SAFire was mounted on the towyo package from September 29 to October 1, 1994. The SAFire has six excitation (Ex) wavelengths (228, 265, 375, 435, 485, and 520 nm) and 16 emission (Em) wavelengths (228, 245, 265, 313, 340, 365, 400, 430, 470, 510, 540, 590, 630, 700, 810, and 900 nm), all with 20 nm FWHM. SAFire fluorescence data were used only qualitatively, since the instrument was not calibrated.

2.4. Nutrient and Particle Analyses

Nutrient concentrations in seawater samples were measured with an Alpkem RFA-300 autoanalyzer in batch mode [*Sakamoto et al.*, 1990].

Flow cytometry analysis was performed on a Coulter Electronics, EPICS 753 flow cytometer [*Campbell et al.*, 1997]. Flow cytometry provided concentration estimates of *Synechococcus* cyanobacteria, *Prochlorococcus* procaryotes, and heterotrophic bacteria from seawater samples collected in situ, and concentrations of heterotrophic bacteria in undiluted sewage samples.

A particle size analyzer (CILAS, France [*Gentien et al.*, 1995]) was added to the platform for two casts on September 29, 1994, and was otherwise used as a bench-top instrument with Niskin bottle samples or sewage samples from the treatment plant. The instrument analysis program derives an estimate in a.u. of the total volume occupied by particles, called particle load, from the transmission of a laser beam (820 nm) through a 3-cm path length cell. After crossing the

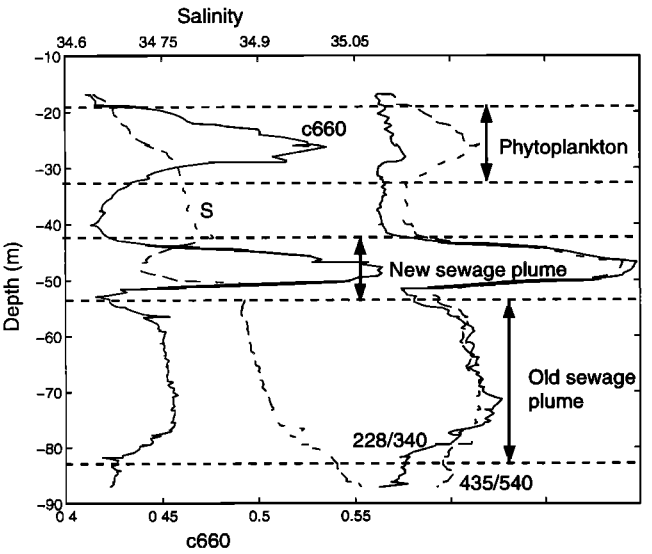

Figure 2. Profiles of salinity, beam attenuation coefficient at 660 nm (c660), and fluorescence, in arbitrary units, for Ex/Em = 228/340 nm and Ex/Em = 435/540 nm. Data are from the second downcast of towyo 32. Three layers were observed: shallow phytoplankton, new and old sewage plumes.

particle suspension, the laser beam provides a diffraction pattern, whose intensity is measured by silicon photodetectors at 17 angles between 0° and 23°. Diffraction intensities are used to determine volume distribution (in percentages) for 30 size classes with upper size limits from 0.7 to 400 μm, using an algorithm based on Fraunhöfer diffraction equations for spherical particles [*Gentien et al.*, 1995]. Full Mie theory could be used to refine the results for particles smaller than 2.56 μm but was not applied here, since interest focused on larger particles. The size distribution in a.u., that is, the relative numerical concentration of particles as a function of particle diameter, is calculated from the volume distribution by dividing each volume percentage by the mean volume of that size class, defined as the spherical volume of a particle, with diameter equal to the midpoint between the extremes of the size class. The density function of size distribution, $F(D)$, is obtained by dividing the size distribution by the width of each size class which increased logarithmically with size.

3. Results

Before describing the biology, optical characteristics, and particle size distributions at the site, it is useful to subdivide the water column vertically into layers affected or not affected by discharged effluent.

3.1. Effect of Discharged Effluent

Up to four layers could be distinguished in the water column, two affected by sewage (recently discharged ("new") sewage plume waters and "old" plume waters) and two unaffected by effluent (shallow and deep phytoplankton layers). Recently discharged or new sewage plume waters were recognized by strong decreases in salinity and increases in c660 (Figure 2). Old sewage plume waters were observed on October 1, 1994, and were characterized by the same signals as new sewage plume waters (low salinity signal, high c660) but smaller in magnitude (Figure 2). This particle field was considered to be older than the sewage plume layer above, since (1) it was deeper and more diluted than new sewage plume; and (2) isopycnal surfaces were rising during the few hours prior to data collection [*Jones et al.*, 1995], so that the old plume would be expected to be deeper than recently discharged effluent. Phytoplankton fields were characterized by increased absorption and beam attenuation coefficients and increased chlorophyll fluorescence compared to clearer waters. One phytoplankton component was located close to the surface; the other one was deeper in the water column near the base of the euphotic zone (Figures 2 and 3). The c660 versus salinity plots have previously provided clear partitioning of the various particle components (*Washburn et al.* [1992]; in conjunction with chlorophyll fluorescence

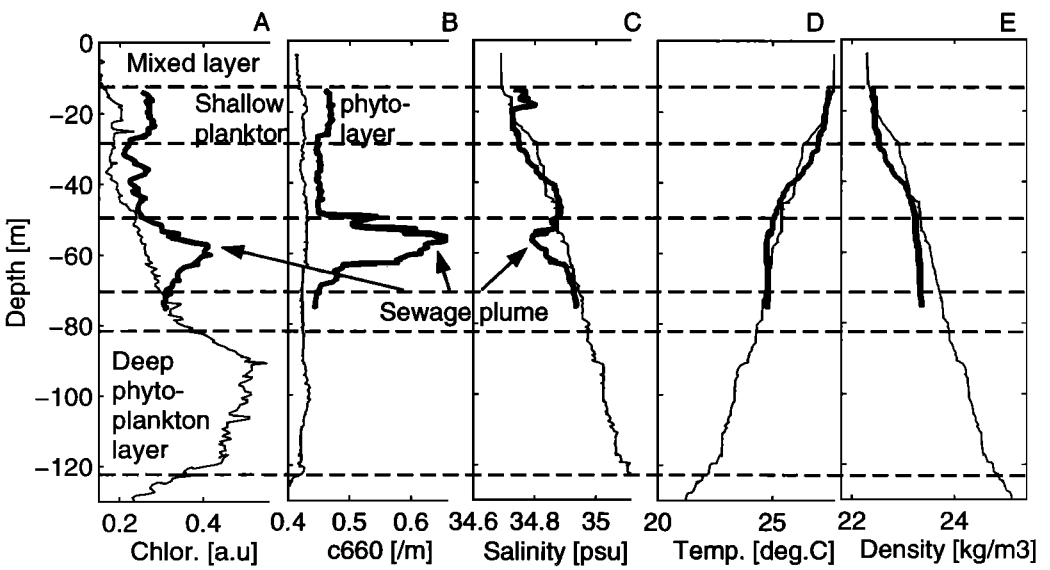

Figure 3. (a) Chlorophyll fluorescence, (b) beam attenuation coefficient at 660 nm (c660), (c) salinity, (d) temperature, and (e) density anomaly. Data are shown for cast 9 (thick line) and cast 12 (thin line).

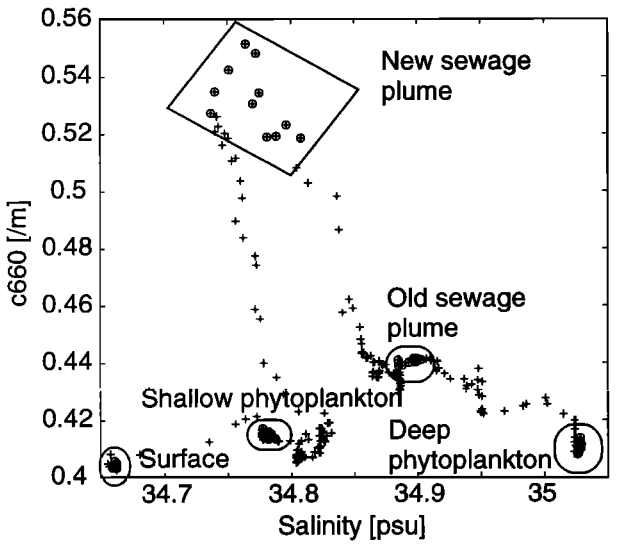

Figure 4. Beam attenuation at 660 nm (c660) versus salinity for towyo 30 (+). The circled crosses indicate the different layers observed in the water column: surface waters, shallow phytoplankton layer, new sewage plume waters, old sewage plume waters, and deep phytoplankton layer.

observations [*Wu et al.*, 1994]) (Figure 4). Surface data were included for comparison. The highest c660 values were associated with new sewage. The magnitude of these parameters varied from day to day, but the relations between the different particle fields were maintained. These types of plots provided greater contrast and allowed better discrimination among the different particle fields than profile plots.

3.2. Inherent Optical Properties

The consistency between the two beam attenuation measurements, c660 and ac-9 data, was checked and showed that the c values from the ac-9 (interpolated between 650 and 676 nm) were 80% higher than $(c\text{-}c_w)(660)$ (c660 with pure water subtracted). Only the absolute values of c660 from the Sea Tech instrument and relative values for a, b, and c from ac-9 measurements were used in our analysis.

3.2.1. **Absorption spectra.** Sewage plume particulate and detrital absorptions at 55 m in cast 9 were larger than corresponding absorptions in the shallow (10 m) phytoplankton layer (Figures 5a and 6a). The DOM signal was stronger in the sewage waters than in the shallow phytoplankton layer for the near ultraviolet (UV), and of the same magnitude for the 450-800 nm range (Figure 5b). Total absorption was stronger at 55 m than at 10 m throughout the UV and visible spectra. Total absorption difference spectra from bench-top spectrophotometric measurements were compared with ac-9 measurements and excellent agreement was obtained, especially at short wavelengths (Figure 5b).

3.2.2. Scattering and spectral slopes. Both scattering and beam attenuation coefficients were higher in the plume than in the phytoplankton fields (Figure 6). The contribution of scattering to beam attenuation increased in plume waters compared with the phytoplankton layers. For cast 9, c412 was 207% higher in the plume than in the shallow phytoplankton layer (10 m), while a412 increased by only 71%. The larger increase in c412 is therefore accounted for by a larger (296%) increase in b412 due to the presence of wastewater. Scattering spectra features, which usually cancel out absorption features, were quite flat, since ac-9 absorption spectra were flatter than traditional phytoplankton, DOM, or detrital absorption spectra (Figures 6a and 6b). Effluent

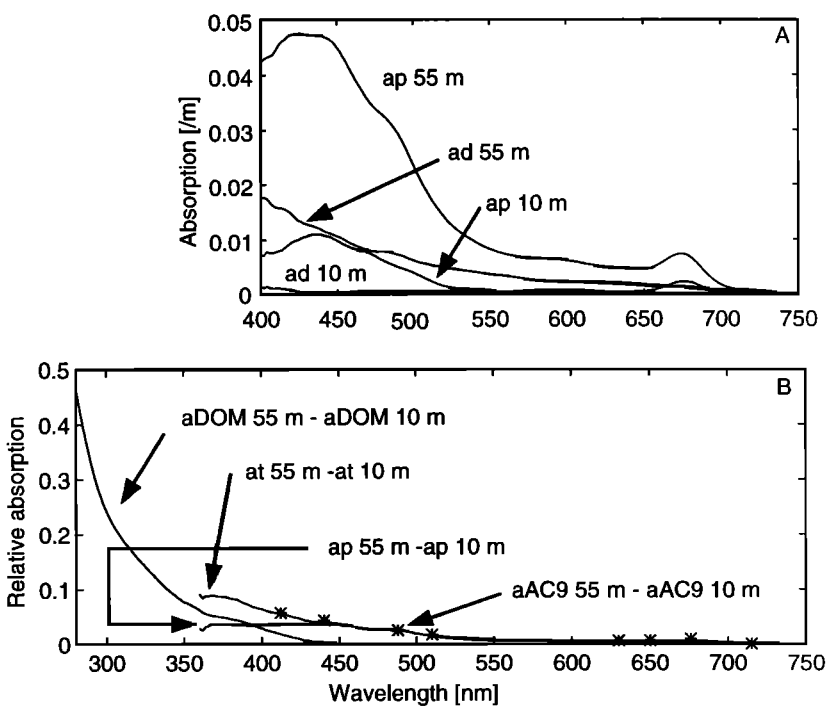

Figure 5. (a) Particulate and detrital absorption spectra at 10 m and 55 m. (b) Relative dissolved organic matter (DOM), particulate, and total (DOM + particulate) and ac-9 (asterisks) absorption spectra between 55 m and 10 m. All data are from cast 9.

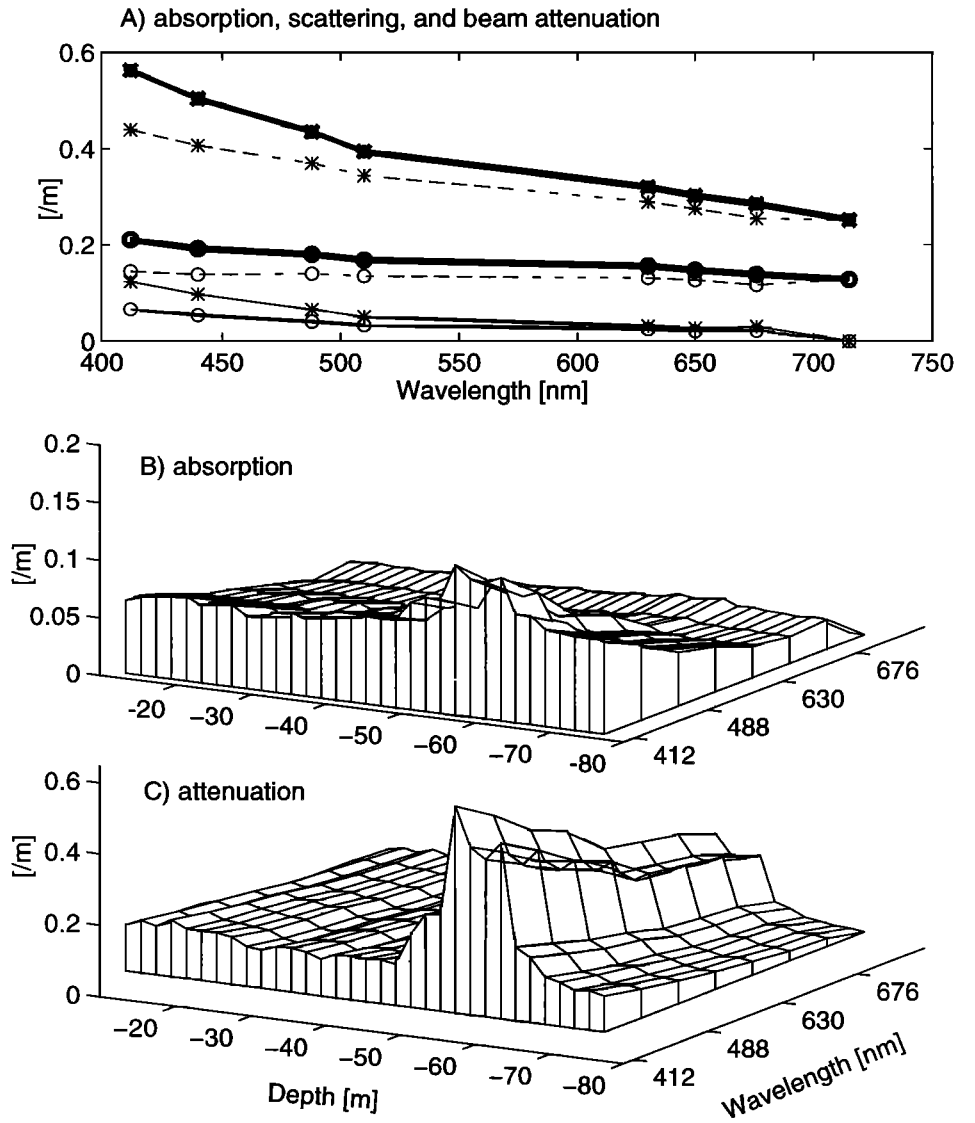

Figure 6. (a) Absorption (thin), scattering (dashed), and beam attenuation (thick) coefficients for eight wavelengths (412, 440, 488, 510, 630, 650, 676, and 715 nm) at 10 m (circles) and 50 m (asterisks) depths. (b) Absorption coefficient (same wavelengths as Figure 6a) versus depth. (c) Same as Figure 6b for beam attenuation coefficient. All data shown are for cast 9.

scattering and beam attenuation spectra did not contain any peculiar peaks and had steep slopes (with a break in the shape around 500 nm), decreasing with increasing wavelength (Figures 6a and 6c). Between 412 and 715 nm, scattering spectra were fit by $\lambda^{-1.0}$ (r^2 = 0.99) in the sewage plume compared to $\lambda^{-0.3}$ (r^2 = 0.77) at 10 m, and attenuation spectra by $\lambda^{-1.4}$ (r^2 = 0.99) in the sewage plume compared to $\lambda^{-0.8}$ (r^2 = 0.97) at 10 m. In the plume the relative contributions of scattering to attenuation increased from 80% at 412 nm to 92% at 650 nm.

3.3. Fluorescence

Throughout the plume, the chlorophyll fluorescence either increased with depth as if the plume was not present (e.g., cast 13; Figure 7), or increased noticeably, peaking at the maximum concentration of the sewage plume (e.g., cast 9; Figure 3).

SAFire fluorescence data were analyzed to determine which Ex/Em wavelength pairs had the strongest and most reliable signals in the presence of sewage plume waters. Ex/Em = 228/340 nm was the best indicator of both new and old sewage plumes, since it increased in the presence of sewage waters but not phytoplankton (Figure 2). Ex/Em = 435/540 nm detected new plume but also the shallow phytoplankton layer when its signature was very strong (Figure 2). Ex/Em = 435/540 nm showed a slight increase in fluorescence in the old sewage plume.

3.4. Nutrient and Particle Characterization

3.4.1. Nutrients. Outside of the sewage plume, nutrient concentrations were typical of oligotrophic waters (Figure 8). Ammonium, silicate, and phosphate concentrations in the sewage plume were at least 2 times greater than in background waters. SITP wastewater was shown to contain high concentrations of phosphate (57 μm), nitrate (2.7 μm), and silicate (556 μm) [*Fujioka and Loh*, 1995]. Dilutions, calculated from wastewater concentrations and nutrient

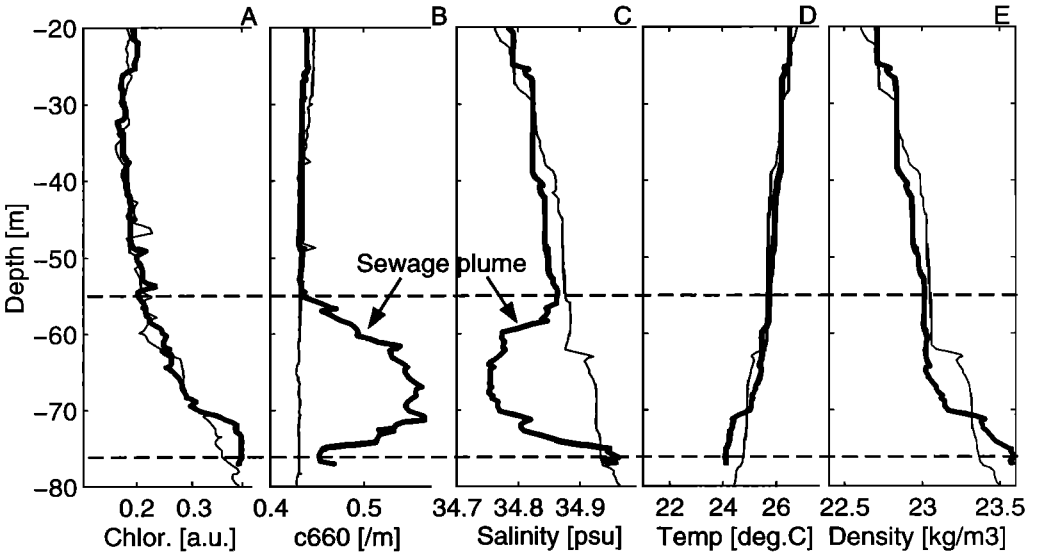

Figure 7. (a) Chlorophyll fluorescence, (b) beam attenuation coefficient at 660 nm (c660), (c) salinity, (d) temperature, and (e) density anomaly. Data are shown for cast 13 (thick line) and cast 15 (thin line). Sewage plume was present at cast 13 but not at cast 15; nonetheless, chlorophyll fluorescence signals were similar for both casts.

anomalies found in the plume, ranged between 1:170 and 1:260 for silicate and phosphate concentrations. This is in agreement with other dilution calculations [*Petrenko et al.*, 1997a] and shows that the plume was much less dilute compared to surfacing plumes (dilution > 1:1000) [*Roberts*, 1995].

3.4.2. Pigments. Chlorophyll *b* (chl *b*) and 19'-hexanoyloxyfucoxanthin (hex) were the dominant carotenoids, followed either by fucoxanthin (fu) in the upper part of the water column (top 30 m) or by 19'-butanoyloxyfucoxanthin (bu) deeper than 35 m [*Petrenko*, 1997]. Offshore of the diffuser (station B), these carotenoids peaked in the deep

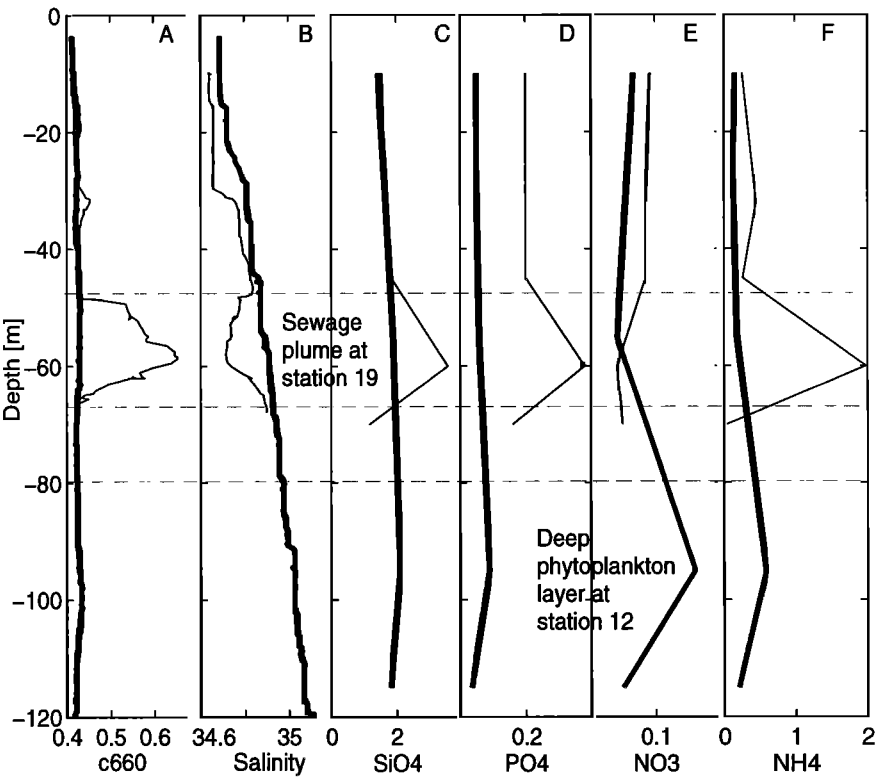

Figure 8. (a) Beam attenuation coefficient at 660 nm (c660) for cast 12 (thick line) and cast 19 (thin line). (b) Same as Figure 8a for salinity. (c-f) Same as Figure 8a for silicate, phosphate, nitrate, and ammonium concentrations in mM.

phytoplankton layer, exhibiting pigment vertical profiles typical of the open ocean. Chl *b* is usually indicative of prochlorophytes and/or green algae [*Lewin*, 1976]. Since violaxanthin, which is indicative of eukaryotic green algae [*Jeffrey*, 1961], was not present accompanying chl *b*, prochlorophytes probably contributed to most of the chl *b*. Hex, fu, and bu contribute to chrysophytes, prymnesiophytes, and diatoms in different proportions. To a first-order approximation, one can consider that hex is indicative of prymnesiophytes, fu of diatoms, and bu of chrysophytes [*Laws and Ziemann*, 1995]. Hence the microalgal communities were composed of prochlorophytes, prymnesiophytes, and either diatoms above 35 m or chrysophytes in the lower part of the water column. No significant changes in the phytoplankton pigment composition were observed in sewage-affected waters. Given the high levels of silicate (up to 3.5 μM) present in the plume, it was expected that the relative proportion of diatoms would increase, but this was not the case since fucoxanthin was low relative to other pigments in the plume [*Jeffrey*, 1961; *Letelier et al.*, 1993]. In effluent enrichment studies (i.e., adding 24-hour composite of wastewater from the treatment plant to water collected in Mamala Bay), *Laws and Ziemann* [1995] found that the dominant carotenoid of sewage-enriched waters was fucoxanthin, and that 19'-hexanoyloxyfucoxanthin relative concentration was small. They did not find such results in pigment analyses performed on in situ samples collected in or around the plume. This corroborates the present study, confirming the lack of significant phytoplankton pigment changes in sewage-affected waters.

3.4.3. Flow cytometry. *Prochlorococcus* median count was 134×10^3 mL^{-1} (range 89.2 - 143.5×10^3 mL^{-1}) in the upper 25 m. *Prochlorococcus* concentration peaked to a median count of 174×10^3 mL^{-1} (range 151.5 - 255×10^3 mL^{-1}) between 55 and 70 m, whether effluent was present (cast 9 and cast 13) or not (cast 12). Offshore (cast 12) *Prochlorococcus* concentration dropped from 255×10^3 mL^{-1} at 55 m to a minimum of 43×10^3 mL^{-1} at the deeper sampled depth (115 m).

Counts of *Synechococcus* cyanobacteria were high at the surface with a median count of 15.4×10^3 mL^{-1} (range 12.3 - 26.2×10^3 mL^{-1}) and decreased with depth steadily below 25 m, down to 0.4×10^3 mL^{-1} at 115 m offshore. Between 55 and 70 m, *Synechococcus* median count was 7.6×10^3 mL^{-1}. Profiles of *Synechococcus* did not contain any features associated with the presence of effluent.

Between 55 and 70 m, heterotrophic bacteria median count was 9.7×10^3 mL^{-1}, while in the rest of the water column it was 6.6×10^3 mL^{-1} (same median count in the surface layer). Heterotrophic bacteria reached their highest concentration (11.5×10^3 mL^{-1}) in the sewage plume at 55 m (cast 9). The offshore cast showed a maximum of 9.5×10^3 mL^{-1} heterotrophic bacteria at 55 m.

Undiluted sewage samples, collected directly from the sewage treatment plant basin, had a median count of 165×10^3 mL^{-1} heterotrophic bacteria for the three collected samples, with an average of 151×10^3 mL^{-1} heterotrophic bacteria for the two morning samples and a peak at 235×10^3 mL^{-1} for the afternoon sample. Sewage samples also exhibited high concentrations of particles with similar size (around 1.2 μm), and fluorescence (Ex/Em = 228/450 nm, 488/575 nm, and 488/680 nm) as *Synechococcus*.

3.4.4. Particle loads, volume, and size distributions. These data corroborated the presence of different horizontal layers and provided additional information.

Table 2. Loads and Percentages, in Volume Distribution, of Three Size Classes: Diameter Smaller Than 45 μm, 45 - 70 μm, and 70 - 260 μm at Each Sampled Depth of Cast 19 and for an Undiluted Sewage Sample (Average of Results of Three Samples Collected at the Treatment Plant)

		Size		
Depth	Load	≤ 45 μm	>45 to ≤ 70 μm	>70 μm
10 m	27	34	6	60
32 m	34	38	28	34
45 m	16	51	39	10
60 m	90	22	1	77
70 m	33	52	5	43
Sewage	6920	87	2	11

3.4.4.1. Particle loads: On September 29, the particle loads, measured in situ with the CILAS analyzer, were in the range 8.5 - 23 a.u. in the water column from 5 to 50 m. The particle loads, measured in the laboratory from Niskin bottle samples collected during cast 19 on October 1, were between 16.5 and 33.5 a.u. in the upper water column (5 - 50 m), 90 a.u. in the sewage plume at 60 m, and 33 a.u. below it at 70 m (Table 2). These data showed that there was a 2.7- to 5.5-fold increase in particle load in the plume compared with surrounding waters. The very low particle loads (especially relative to loads measured in European coastal waters [*Gentien et al.*, 1995]) indicate that the Mamala Bay background waters were relatively oligotrophic during the cruise.

3.4.4.2. Particle volume distributions: On October 1 the volume distributions exhibited weaker bimodal distributions at depths of 32 and 45 m than in the rest of the water column (Table 2). The two modes of particles were the "small particles" (diameter ≤ 45 μm) and the "large particles" (diameter > 70 μm). Compared to the rest of the water column, sewage had a small volume (1%) of "medium particles" (45 < diameter ≤ 70 μm) (Table 2). A comparable small volume of medium particles (2%) was found in treated sewage samples.

3.4.4.3. Size distributions: The density functions of size distribution, $F(D)$, were flatter at 32 and 45 m than at 10, 60, and 70 m (data not shown), reflecting the degree of bimodality observed in the volume distributions. The slopes of the log-log plots varied from -3.2 for particles smaller than 10 μm to -13 for particles larger than about 100 μm. The sewage plume (60 m) $F(D)$ had more particles smaller than 40 μm and larger than 70 μm than background waters (Figure 9). The 70 m $F(D)$ was similar to the 60 m $F(D)$ with slightly fewer large particles but still more than background concentration (data not shown).

4. Discussion

4.1. Impacts of Sewage on Microorganisms

The impacts of the Sand Island sewage outfall on biology, optical characteristics, and particle size distributions were examined around the end of the outfall diffuser. Chlorophyll fluorescence within the plume exceeded that in surrounding waters in conditions characterized by low Froude numbers (Fr about 0.1), while chlorophyll fluorescence within the plume was equivalent to that outside the plume when the Froude number was high (Fr about 6) [*Petrenko et al.*, 1997a]; Froude

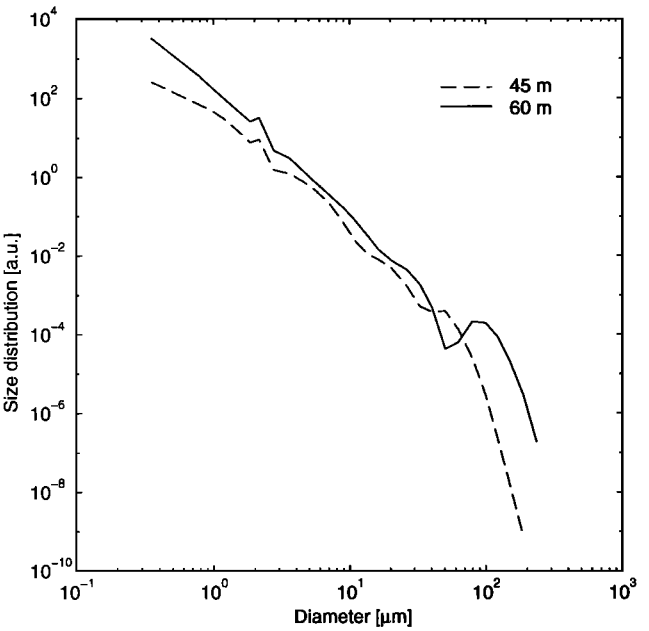

Figure 9. Size distribution versus diameter for seawater samples collected above the sewage plume (45 m) and in the sewage plume (60 m) at cast 19.

number is defined as Fr = u^3/B, where u is the horizontal velocity and B is the specific wastewater buoyancy flux per diffuser length [e.g., *Roberts*, 1977]. If the change in chlorophyll fluorescence is assumed to reflect a change in phytoplankton concentration and growth, these observations are consistent with previous findings that sewage stimulates the growth of phytoplankton when the timescale of plume dilution is longer than phytoplankton growth response [*Thompson and Ho*, 1981]. This highlights the importance of the physical forcing on the plume and phytoplankton interactions. In sewage-enriched waters, *Laws and Ziemann* [1995] found an increase of 60% in phytoplankton photosynthetic rates after 24 hours at dilution of 1:1000.

Pigment analysis demonstrated no significant change in the phytoplankton community in the presence of effluent compared with what would be expected for sewage-enriched waters. Flow cytometry analysis showed increases of 30% in heterotrophic bacteria concentration and high concentrations of *Prochlorococcus* (also observed in pigment analysis), not only in the plume but also at plume depths offshore. It is not clear whether the high counts of heterotrophic bacteria and *Prochlorococcus* at 55 m offshore were due to natural distributions of these populations in the water columns or were remnants of past plume influence at that depth. Horizontal currents, at the depths of the sewage plume and below, were southward earlier that day (during two periods, 0000 - 0200 and 1300 - 1400 UT) and could have advected the plume offshore [*Jones et al.*, 1995]. No variations in concentration associated with the presence of effluent were observed for *Synechococcus* cyanobacteria. Those measurements differed from those made at White's Point, California, where high concentrations of *Synechococcus* were associated with the sewage plume [*Iturriaga et al.*, 1990].

Around sewage outfalls, flocculation and coagulation result in deposition of metals and dense particles, while flotables and grease rise to the surface. The sample taken in the plume had the volume proportion of medium size (45 - 70 μm) particles that was most similar to that of sewage samples from the treatment plant (1% versus 2%). In the plume there were more large particles (> 70 μm) than in background waters. Some large particles were present in sewage, while others probably originated from flocculation and coagulation of smaller effluent particles once the wastewater was injected into the water column [e.g., *Johnson et al.*, 1994; *Newman et al.*, 1990; *Schulz et al.*, 1994]. These large particles appeared to sink close to the diffuser, since they were also detected below the plume at the western end of the diffuser. This observation suggests deposition of effluent particles and potential accumulation of metals and other contaminants in sediments close to the diffuser [e.g., *Klein and Goldberg*, 1970]. During the cruise, no flotables or changes in surface appearance (grease slicks) were detected, probably because the stratification acted to trap the lighter effluent components at depth.

The effects of the plume listed above were observed mainly at the western end of the diffuser for initial dilutions of about 1:250. Since these dilutions are small compared to the initial dilutions generally predicted at the Sand Island diffuser [*Roberts*, 1995], the impacts described above are likely to represent the upper limits of effluent impacts in our study area. Internal tides were shown to displace the plume vertically [*Petrenko et al.*, 1997b] and could move the deeply trapped (hence relatively low dilution) sewage plume to a shallower depth, potentially bringing contaminants into swimming waters. In this latter case or in the case of surfacing plumes, biological and optical impacts different than those observed in this study are expected.

4.2. Potential Techniques to Monitor Sewage

During the cruise, the plume was trapped at depth, with smaller dilutions (about 1:250) than if it had been surfacing, and hence was detectable in real-time by its characteristic signatures of low salinity and high c660. However, in many cases, such signatures may be undetectable. For example, large gradients in background salinity or c660 could obscure the signature of the plume. A surfacing plume, which could be 5 times as dilute as a submerged plume, would be surrounded with low-salinity surface waters having potentially high c660 values associated with a shallow phytoplankton layer. In this case the salinity and c660 signatures may not be readily distinguishable from the surface signature. In summary, salinity and c660 were good in situ and real-time detectors of the main body of the plume during this cruise but may not always serve as reliable plume tracers.

Fluorescence at Ex/Em = 228/340 nm may provide another unique signature for the sewage plume, since it did not correlate with phytoplankton fields. Plumes can be either trapped or surfacing. In contrast with c660, fluorescence at Ex/Em = 228/340 nm has the advantage that it does not increase in phytoplankton layers and, in contrast with salinity, that it does not decrease with shallower depths. Hence fluorescence at Ex/Em = 228/340 nm may be a more promising technique than the traditional natural tracers c660 and salinity for detection of both trapped and surfacing plumes.

In laboratory experiments, fluorescence at Ex/Em = 228/340 nm was associated with the presence of aromatic amino acids, either free or as protein constituents, so this Ex/Em signal is referred to as protein-like fluorescence [*Wolbeis*, 1985]. For example, *E. coli*'s tryptophan has been shown to exhibit strong signals at such a wavelength pair [*Bronk and*

Reinisch, 1993]. Wastewaters can contain numerous types of chromophores, including humic substances, phenols, steroids, oils, nonvolatile acids, and detergents, so that their absorption and fluorescence spectra are likely to contain broad features rather than specific peaks. However, as mentioned earlier, *Ahmad et al.* [1993] found one chromophoric group excited at 248 nm in raw sewage with an emission maximum around 340 nm. The maximum emission of secondary-treated wastewater, for excitation at 248 nm, occurred around 450 nm [*Ahmad and Reynolds*, 1995]. In the present study, Ex/Em = 228/340 nm was a better detector of sewage plume than Ex/Em = 228/430, 228/470, 265/340, 265/430, and 265/470 nm. Additional laboratory experiments on sewage samples from other locations should be pursued, and field work with a calibrated SAFire should be done in order to define the wavelength pairs most appropriate for particular sewage water detection. Fluorescence at Ex/Em = 228/340 nm has been observed in sediments or marine waters by others (among the most recent works are *Coble* [1996], *Cowles et al.* [1996], *Desiderio et al.* [1996], *Determan et al.* [1996]), and has been interpreted as particulate tryptophan-like fluorescence [*Determan et al.*, 1996]. Any living material containing tryptophan, especially bacteria [*Determan et al.*, 1996], is likely to fluoresce at this wavelength pair, but the amplitude of the signal and/or signals at other wavelengths could probably be used to differentiate between fluorescing compounds.

Up to now, in situ and real-time detection of old plume waters has only been done by adding tracers [*Faisst et al.*, 1990] or using acoustic methods [*Dammann et al.*, 1991]. But tracer techniques are intrusive and costly methods, which involve intensive preparation (adjustment of tracer buoyancy and coagulation efficiency, dilution of tracer, coordination with cruise time), and acoustic methods can be imprecise due to background signals. In this study the detection of old plume waters provided the opportunity to check whether instruments such as the SAFire, never used before in sewage plume studies, could detect the old sewage plume. Ex/Em = 228/340 nm was a good indicator of the old plume; it showed detection comparable to the c660 signal during our measurements (Figure 2). Once calibrated, fluorescence at Ex/Em = 228/340 nm may prove to be a good tracer of old sewage plumes.

Scattering and beam attenuation coefficients and their respective spectral slopes were greater in the sewage plume than in the rest of the water column. Increase in scattering, due to the presence of effluent, is responsible for nonnegligible decreases in downwelling radiant flux [*Petrenko et al.*, 1994] and could generate increases in water-leaving reflectance for shallow water outfalls. Absolute values of a, b and c would permit the development of spectral algorithms for in situ detection of effluent and remote detection of surfacing sewage plumes.

5. Conclusion

Inputs of primary-treated sewage resulted in significant effects on the biology, optical characteristics, and particle size distributions close to the diffuser. Increases of (1) chlorophyll fluorescence for low Froude number, (2) nutrients, (3) particulate tryptophan-like fluorescence, (4) scattering coefficients in the visible range, and (5) particle loads are expected to be observed at other outfall diffusers and can be used to interpret sewage plume dispersion in coastal waters. These effects are expected to be qualitatively similar at other sewage diffusers but quantitatively different, depending on the wastewater composition and ambient oceanographic conditions. Since the plume was trapped at depth with initial dilution around 1:250 during our measurements, it is expected that reduced effects would be observed if the plume were surfacing, since its dilution would then be much higher.

Effluents differ, depending on the type of treatment used and, once in the water, on their dilution and the type of background waters with which they mix. Further effort should be directed toward characterizing the optical variability associated with such factors in order to test the potential of SAFire fluorescence measurements as a noninvasive real-time in situ technique to detect sewage fields in coastal environments.

Acknowledgments. Funding for this research was made possible by grants from the Mamala Bay Study Commission Fund, a component trust of Hawaii Community Foundation, and by additional grants from USC Sea Grant. We thank Derek Manov, David Foley, Jerry Wiggert, the personnel of the Marine Center of Hawaii, and the crew of the R/V *Kila* for their help during the hydrographic cruise. We are grateful to Zhihong Zheng, Lisa Campbell, Hector Nolla, Bob Bidigare, Mike Ondrusek, Mikel Latasa, and Dave Karl for sample analyses or assistance. Special thanks go to Dariusz Stramski, Ricardo Letelier, and David Adelson for reviewing the manuscript.

References

Ahmad, S.R., and D.M. Reynolds, Synchronous fluorescence spectroscopy of wastewater and some potential constituents, *Water Res.*, *29* (6), 1599-1602, 1995.

Ahmad, S.R., V.G. Foster, and D. Reynolds, Laser scattering technique for non-invasive analysis of waste water, in *Substance Detection Systems*, pp. 353-359, Soc. of Photo-Opt. Instrum. Eng. (SPIE), Bellingham, Wash., 1993.

Bartz, R., R. Spinrad, and J.C. Kitchen, A low power, high resolution, in situ fluorometer for profiling and moored applications in water, *Ocean Opt.*, *9*, 157-170, 1988.

Besiktepe, S.T., E. Ozsoy, and M.A. Latif, Sewage outfall plume in the 2-layer channel - An example of Istanbul outfall, *Water Sci. Technol.*, *32* (2), 69-75, 1995.

Bricaud, A., and D. Stramski, Spectral absorption coefficients of living phytoplankton and nonalgal biogenous matter: A comparison between the Peru upwelling area and the Sargasso Sea, *Limnol. Oceanogr.*, *35* (3), 562-582, 1990.

Bronk, B.V., and L. Reinisch, Variability of steady-state bacterial fluorescence with respect to growth-conditions, *Appl. Microsc.*, *47* (4), 436-440, 1993.

Campbell, L., H. Liu, H.A. Nolla, and D. Vaulot, Annual variability of phytoplankton and bacteria in the subtropical North Pacific Ocean at Station ALOHA during the 1991-1994 ENSO event, *Deep Sea Res.*, *44* (2), 167-192, 1997.

Coble, P.G., Characterization of marine and terrestrial DOM in seawater using excitation-emission matrix spectroscopy, *Mar. Chem.*, *51*, 325-346, 1996.

Colwell, R.R., G.T. Orlob, and J.R. Schubel, Study management, *Rep. MB-1*, Mamala Bay Comm., Oahu, Hawaii, 1995.

Cowles, T.J., J.R.V. Zaneveld, R.A. Desiderio, S. Pegau, and C. Moore, In situ estimation of DOM using multi-excitation spectral fluorescence and absorption, *Eos Trans. AGU*, *77* (3), Ocean Sci. Meet. Suppl., 1996.

Dammann, W.P., J.R. Proni, J.F. Craynock, and R. Fergen, Oceanic wastewater outfall plume characteristics measured acoustically, *Chem. Ecol.*, *5*, 75-84, 1991.

Davison, A., P. Thornton, and G. Spelman, The dispersion of sewage from the deep water outfall off Malabar using radioisotope tracer techniques, Rep. Interim EPA, Aust. Nucl. Sci. and Technol. Organ. Menai, N.S.W., 1993.

Desiderio, R.A., T.J. Cowles, J.R.V. Zaneveld, and C. Moore, Multi-excitation spectral absorption and fluorescence: a new in situ device

for characterizing dissolved and particulate material, *Eos Trans. AGU, 77* (3), Ocean Sci. Meet. Suppl., 1996.

Determan, S., R. Reuter, and R. Willkomm, Fluorescent matter in the eastern Atlantic Ocean, Part 2, Vertical profiles and relation to water masses, *Deep Sea Res., 43* (3), 345-360, 1996.

Faisst, W.R., M. McDonald, T. Noon, and G. Marsh, Iona outfall, plume characterization study, in *Proceedings 1990 National Conference on Hydraulic Engineering*, edited by H. Chang, Am. Soc. of Civ. Eng., New York, 1990.

Fujioka, R.S., and P.C. Loh, Characterization of the microbiological quality of water in Mamala Bay, *Rep. MB-7*, Mamala Bay Comm., Oahu, Hawaii, 1995.

Gentien, P., M. Lunven, M. Lehaitre, and J.L. Duvent, In-situ depth profiling of particle sizes, *Deep Sea Res., 42* (8), 1297-1312, 1995.

Holm-Hansen, O., C.J. Lorenzen, R.W. Holmes, and J.D.H. Strickland, Fluorometric determination of chlorophyll, *J. Cons. Perm. Int. Explor. Mer, 30*, 3-15, 1965.

Iturriaga, R.H., R. Bartz, and J.R. Zaneveld, In-situ active fluorometer to measure coccoid cyanobacteria fluorescence, Ocean Opt. X, *Proc. SPIE Int. Soc. Opt. Eng., 1302*, 346-354, 1990.

Jeffrey, S.W., Paper-chromatographic separation of chlorophylls and carotenoids from marine algae, *Biochem. J., 80*, 336-342, 1961.

Johnson, B.D., K. Kranck, and D.K. Muschenheim, Physicochemical factors in particle aggregation, in *The Biology of Particles in Aquatic Systems*, edited by R.S. Wotton, Lewis Publishers, Boca Raton, Fla, 1994.

Jones, B.H., A. Bratkovich, T.D. Dickey, G. Kleppel, A. Steele, R. Iturriaga, and I. Haydock, Variability of physical, chemical, and biological parameters in the vicinity of an ocean outfall plume, in *Stratified Flows: Proceedings of the Third International Symposium on Stratified Flows*, edited by E.J. List and H.H. Jirka, pp. 877-890, Am. Soc. of Civ. Eng., New York, 1990.

Jones, B.H., L. Washburn, and Y. Wu, The dispersion of ocean outfall plumes: physical and biological dynamics, in *Coastal Zone '91, Proceedings of 7th Symposium on Coastal and Ocean Management*, pp. 74-85, Am. Soc. of Civ. Eng., New York, 1991.

Jones, B.H., T.D. Dickey, L. Washburn, and D. Manov, Physical and biological dynamics of sewage outfall plumes in the coastal region: An integrated observational approach, in *Water Pollution II: Modeling, Measuring and Prediction*, edited by L.C. Wrobel and C.A. Brebbia, pp. 527-534, Comput. Mech. Publi., Southampton, England, 1993.

Jones, B.H., T.D. Dickey, and A.A. Petrenko, Plume dynamics and dispersion in Mamala Bay, HI, *Rep. MB-S11*, Mamala Bay Comm., Oahu, Hawaii, 1995.

Kishino, M., M. Takahashi, N. Okami, and S. Ichimura, Estimation of the spectral absorption coefficients of phytoplankton in the sea, *Bull. Mar. Sci., 37* (2), 634-642, 1985.

Klein, D.H., and E.D. Goldberg, Mercury in the marine environment, *Environ. Sci. Technol., 4*, 765-768, 1970.

Laws, E.A., *Aquatic Pollution*, 611 pp., Wiley-Interscience, New York, 1993.

Laws, E.A., and D. Ziemann, Ecosystem response study: Effects of sewage discharges and stream runoff on phytoplankton communities and water quality in Mamala Bay, *Rep. MB-9*, Mamala Bay Comm., Oahu, Hawaii, 1995.

Letelier, R.M., R.R. Bidigare, D.V. Hebel, M.C. Ondrusek, D. Winn, and D.M. Karl, Temporal variability of phytoplankton community structure based on pigment analysis, *Limnol. Oceanogr., 38* (7), 1420-1437, 1993.

Lewin, R.A., Prochlorophyta as a proposed new division of algae, *Nature, 261*, 697-698, 1976.

Mitchell, B.G., and D.A. Kiefer, Determination of absorption and fluorescence excitation spectra for phytoplankton, in *Marine Phytoplankton and Productivity*, edited by L. Bollis and R. Gilles, pp. 157-169, Springer-Verlag, New York, 1984.

Mitchell, B.G., and D.A. Kiefer, Chlorophyll *a* specific absorption and fluorescence excitation spectra for light-limited phytoplankton, *Deep Sea Res., 35*, 639-664, 1988.

Moore, C., J.R.V. Zaneveld, and J.C. Kitchen, Preliminary results from an in-situ spectral absorption meter, Ocean Opt. XI, *Proc. SPIE Int. Soc. Opt. Eng., 1750*, 330-337, 1992.

Newman, K.A., S.L. Frankel, and K.D. Stolzenbach, Flow cytometric detection and sizing of fluorescent particles deposited at a sewage outfall site, *Environ. Sci. Technol., 24* (4), 1990.

Parnell, P.E., Impacts to phytoplankton and water quality of Hawaiian coastal waters by primary and secondary sewage outfalls, M.S. thesis, Univ. of Hawaii, Honolulu, 1992.

Pegau, W.S., The effects of physical parameters on the absorption coefficient of natural waters, Ph.D. thesis, Oreg. State Univ., Corvallis, 1996.

Petrenko, A.A., Detection and characterization of the sewage plume at Sand Island, Hawaii, Ph.D. thesis, Univ. of S. Calif., Los Angeles, 1997.

Petrenko, A., D.G. Foley, T.D. Dickey, and B.H. Jones, Spectral analysis of particle fields in the vicinity of a sewage outfall: Comparison of modeled and in situ data, *Eos Trans. AGU, 75* (3), Ocean Sciences Meet. Suppl., 1994.

Petrenko, A.A., B.H. Jones, and T.D. Dickey, Shape and initial dilution of the Sand Island, Hawaii sewage plume, *J. Hydraul. Eng., in press*, 1997a.

Petrenko, A.A., B.H. Jones, T.D. Dickey, and P. Hamilton, Internal tide effects on the sewage plume at Sand Island, Hawaii, *Cont. Shelf Res., in press*, 1997b.

Reynolds, D.M., and S.R. Ahmad, The effect of metal-ions on the fluorescence of sewage wastewater, *Water Res., 29* (9), 2214-2216, 1995.

Roberts, P.J.W., Dispersion of buoyant waste water discharged from outfall diffusers of finite length, Ph.D. thesis, Calif. Inst. of Technol., Pasadena, 1977.

Roberts, P.J.W., Near-field modeling of the Mamala Bay Outfalls, *Water Sci. Technol., 32* (2), 159-166, 1995.

Roberts, P.J.W., and D. Wilson, Field and model studies of ocean outfalls, in *Proceedings 1990 National Conference on Hydraulic Engineering*, edited by H. Chang, Am. Soc. of Civ. Eng., New York, 1990.

Sakamoto, C.M., G.E. Friederich, and L.A. Codispoti, MBARI procedures for automated nutrient analyses using a modified Alpkem Series 300 rapid flow analyzer, *Rep. 90-2*, MBARI, Pacific Grove, Calif., 1990.

Schulz, T.J., P.J. Marczan, and A.G. Fane, Behavior of sewage effluent oil and grease in the ocean, *Water Environ. Res., 66*, 800-804, 1994.

Thompson, C.B., and J. Ho, Some effects of sewage discharge upon phytoplankton in Hong Kong, *Mar. Poll. Bull., 12* (5), 168-173, 1981.

Washburn, L., B.H. Jones, A. Bratkovich, T.D. Dickey, and M.S. Chen, Mixing, dispersion, and resuspension in vicinity of ocean wastewater plume, *J. Hydraul. Eng.*, Am. Soc. of Civ. Eng., *118* (1), 38-58, 1992.

Wolbeis, O.S., The fluorescence of organic natural products, in *Molecular Luminescence Spectroscopy, Part I: Methods and Applications*, edited by S.G. Schuman, pp. 167-370, John Wiley, New York, 1985.

Wu, Y.C., L. Washburn, and B.H. Jones, Buoyant plume dispersion in a coastal environment - Evolving plume structure and dynamics, *Cont. Shelf Res., 14* (9), 1001-1023, 1994.

Zaneveld, J.R.V., J.C. Kitchen, and C. Moore, The scattering error correction of reflecting-tube absorption meters, Ocean Opt. XII, *Proc. SPIE Int. Soc. Opt. Eng., 2258*, 44-55, 1994.

T. D. Dickey, Institute for Computational Earth System Science, University of California Santa Barbara, CA 93106.

B. H Jones, Department of Biological Sciences, University of Southern California, Los Angeles, CA 90089.

M. LeHaitre, Institut Francais de Recherche pour l'Exploitation de la Mer, Centre de Brest, BP 70, 29280 Plouzane, France.

C. Moore, Western Environmental Technology Laboratories, Inc., PO Box 518, Philomath, OR 97370.

A. A. Petrenko, Department of Earth Sciences, University of Southern California, Los Angeles, CA 90089-0740 (petrenko@usc.edu).

(Received October 17, 1996; revised June 27, 1997;
accepted July 24, 1997.)